Supplementary Material: Learning by Aligning Videos in Time

Sanjay Haresh* Sateesh Kumar* Huseyin Coskun Shahram N. Syed
Andrey Konin M. Zeeshan Zia Quoc-Huy Tran

Retrocausal, Inc.
Seattle, WA
www.retrocausal.ai

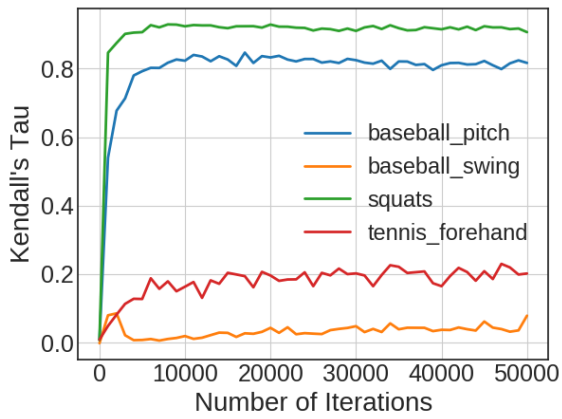

Figure S1: Kendall's Tau results by TCC.

In this supplementary material, we first present results on a subset of 11 actions of *Penn Action* in Sec. 1 and fine-grained frame retrieval results on *IKEA ASM* in Sec. 2. We then show training-from-scratch results in Sec. 3 and ablation results of α, σ, and p in Sec. 4. Next, in Sec. 5 we show results of combining LAV with TCC and TCN while we show results on a recent frame-shuffling method in Sec. 6. Moreover, we visualize our embeddings and provide our labels for *Penn Action* in Secs. 7 and 8 respectively. Finally, we describe our additional implementation details in Sec. 9.

1. Results on a Subset of 11 Actions of *Penn Action*

Among the 3 datasets that we use in Sec. 5 of the main paper (i.e., *Pouring*, *Penn Action*, and *IKEA ASM*), we notice that for *Penn Action* while TCC performs well on most actions, it struggles on 2 actions i.e., *Baseball Swing* and

(a) Baseball Swing

(b) Tennis Forehand

Figure S2: Example alignment errors by TCC. On the left is the reference frame in one video, and on the right is the aligned frame in another video by TCC (i.e., via nearest neighbor search in the embedding space). The frame on the left is among the beginning frames, while the frame on the right in among the ending frames. TCC incorrectly aligns them together due to their similar appearances/poses.

Tennis Forehand. As we can see in Fig. S1, the Kendall's Tau results by TCC on the above 2 actions (red and orange curves) do not go higher than ~ 0.2, which hurts its overall performance on *Penn Action* in Tabs. 2-4 of the main paper. This might be due to the fact that the beginning and ending frames of the above 2 actions are visually similar, and TCC

* indicates joint first author.
{sanjay,sateesh,huseyin,shahram,andrey,zeeshan,huy}@retrocausal.ai

	Method	Classification	Progress	τ
Penn Action	SAL [4]	82.03	0.7054	0.7783
	TCN [5]	82.99	0.7281	**0.8275**
	TCC [2]	83.94	**0.7394**	0.8001
	LAV (Ours)	**84.47**	0.6654	0.8149
	LAV+TCC (Ours)	84.14	0.7111	0.7892

Table S1: Phase classification, phase progression, and Kendall's Tau results on a subset of 11 actions of *Penn Action*. Best results are in **bold**, while second best ones are underlined.

	Method	AP@5	AP@10	AP@15
Penn Action	SAL [4]	76.83	76.52	76.35
	TCN [5]	78.09	77.74	77.52
	TCC [2]	**79.49**	79.19	79.00
	LAV (Ours)	79.34	**79.23**	**79.08**
	LAV + TCC (Ours)	79.29	79.15	79.03

Table S2: Fine-grained frame retrieval results on a subset of 11 actions of *Penn Action*. Best results are in **bold**, while second best ones are underlined.

does not have an explicit mechanism to avoid aligning the beginning frames with the ending ones and vice versa (see Fig. S2 for examples). Other self-supervised methods, i.e., SAL, TCN, and LAV, do not suffer from the above problem as TCC, since they leverage temporal order information, i.e., SAL performs temporal order verification, TCN uses temporal coherence, while LAV exploits both temporal coherence and dynamic time warping prior. Also, the above problem for TCC might be alleviated by tuning the number of context frames and context stride, however, that requires further exploration.

For completeness, we filter out the results of the above 2 actions from Tabs. 2-4 of the main paper, and present the results of the remaining 11 actions of *Penn Action* in Tabs. S1 and S2. From the results, the performance of TCC is improved significantly when excluding the above 2 actions. In Tab. S1, TCC has competitive numbers with TCN and LAV (e.g., TCC performs the best on progression, while TCN and LAV perform the best on Kendall's Tau and classification respectively). In Tab. S2, TCC and LAV have very competitive numbers (e.g., TCC slightly outperforms LAV for AP@5, while LAV marginally outperforms TCC for AP@10 and AP@15), outperforming SAL and TCN.

	Method	AP@5	AP@10	AP@15
IKEA ASM	SAL [4]	15.15	14.90	14.72
	TCN [5]	19.15	19.19	19.33
	TCC [2]	19.80	19.64	19.68
	LAV (Ours)	**23.89**	**23.65**	**23.56**
	LAV + TCC (Ours)	22.95	22.80	22.70

Table S3: Fine-grained frame retrieval results on *IKEA ASM*. Best results are in **bold**, while second best ones are underlined.

	Method	Classification	Progress	τ
Pouring	SAL [4]	85.86	0.6422	0.7329
	TCN [5]	85.98	0.6732	0.7500
	TCC [2]	**88.59**	0.7104	0.7774
	LAV (Ours)	87.70	**0.7320**	**0.7867**

Table S4: Training-from-scratch results on *Pouring*. Best results are in **bold**, while second best ones are underlined.

2. Fine-Grained Frame Retrieval Results on *IKEA ASM*

We now conduct fine-grained frame retrieval experiments on *IKEA ASM* and report the quantitative results of different self-supervised methods in Tab. S3. It is evident from the results that LAV consistently achieves the best performance across different values of K, outperforming other methods by significant margins. For example, for AP@5, LAV obtains 23.89%, while TCC, TCN, and SAL get 19.80%, 19.15%, and 15.15% respectively. Furthermore, the combined LAV+TCC leads to significant performance increase over TCC. For instance, for AP@5, LAV+TCC achieves 22.95%, while TCC obtains 19.80%. The above observations on *IKEA ASM* are similar to those on *Penn Action* and *Pouring* reported in Sec. 5.4 of the main paper, confirming the utility of our self-supervised representation for fine-grained frame retrieval.

3. Training-from-Scratch Results

All of the experiments in Sec. 5 of the main paper utilize an encoder network initialized with pre-trained weights from ImageNet classification. For completeness, we now experiment with learning from scratch. We use a smaller backbone network, i.e., VGG-M [1], (instead of ResNet-50) for this experiment. Tab. S4 shows the quantitative results of different self-supervised methods when learning from scratch on *Pouring*. It can be seen from Tab. S4 that the performance of all methods drops as compared to Tabs. 2 and 3 of the main text. Moreover, SAL and TCN are inferior to TCC and LAV across all metrics. Lastly, although

	Method	Classification	Progress	τ
Penn Action	SAL	64.05	0.2989	0.4145
	TCN	60.17	0.1909	0.4260
	TCC	<u>65.53</u>	**0.4304**	<u>0.4529</u>
	LAV (Ours)	**67.90**	<u>0.3853</u>	**0.4929**

Table S5: Training-from-scratch results on *Penn Action*. Best results are in **bold**. Second best results are <u>underlined</u>.

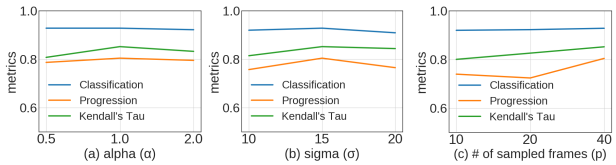

Figure S3: Ablation results of α in (a), σ in (b), and p in (c) on *Pouring*. We convert classification results from % to $[0, 1]$.

LAV has slightly lower classification accuracy than TCC, LAV outperforms TCC on both progression and Kendall's Tau.

Next, Tab. S5 shows training-from-scratch results on *Penn Action*, using a single joint model for all actions (similar as Sec. 5.5 of the main paper). For all methods, the performance in Tab. S5 is lower than Tab. 5 of the main text. Also, SAL and TCN are inferior to TCC and LAV. TCC performs the best on progression, while LAV performs the best on the other two metrics.

Finally, we obtain training-from-scratch results on *IKEA ASM*, which show LAV achieves the best performance (i.e., for classification, **23.84** for LAV vs. **22.04**, **20.45**, and **20.42** for TCC, TCN, and SAL respectively).

4. Ablation Results of α, σ, and p

We first present ablation results of α on *Pouring* in Fig. S3(a). We observe that the performance is generally stable across values of α, and $\alpha = 1.0$ yields the best results. Next, Figs. S3(b) and S3(c) illustrate ablation results of σ and p respectively on *Pouring*. From the results, the performance is generally stable across values of σ and p. Particularly, $\sigma = 15$ performs the best, and large p is preferred.

5. Performance of LAV+TCC and LAV+TCN

We note that LAV+TCC does not consistently perform better than LAV in Tabs. 2 and 3 of the main paper. This might be attributed to the fact that LAV works on L2-normalized embeddings while TCC does not. Since the two components operate on different embedding spaces, combining the two might not always lead to better results.

In addition, we evaluate LAV+TCN on *Pouring*. We notice LAV+TCN suffers from the same problem as LAV+TCC (i.e., normalized/unnormalized embeddings). LAV+TCN obtains **91.22**, **0.7866**, and **0.7925** for classification, progression, and Kendall's Tau respectively, which are comparable to TCN but lower than LAV.

6. Performance of a Recent Frame-Shuffling Method

We evaluate the clip order prediction (COP) method of Xu et. al. [6] on *Pouring*. As it is a clip-based method, we use sliding windows to generate embeddings for frames at window centers. As mentioned in Sec. 4 of the main paper, the network is first trained for the pretext task and then frozen while we train SVM classifier/linear regressor for the main tasks. It achieves **79.44**, **0.5309**, and **0.6656** for classification, progression, and Kendall's Tau respectively, which are lower than SAL in Tabs. 2 and 3 of the main paper. This is likely because the pretext task (i.e., COP) is clip-based, whereas the main tasks are frame-based and require capturing fine-grained frame-based details. Further, since we freeze the network while training SVM classifier/linear regressor, it could not disregard irrelevant clip-based details to focus on the one frame that matters.

7. Visualization of Embeddings

We present the t-SNE visualization [3] of the embeddings learned by LAV on 3 example actions of *Penn Action* in Fig. S4. For each action, we show 4 videos with each plotted using a unique color. In addition, we use different shades of the same color to distinguish different frames of the same video, i.e., beginning frames have light shades, while later frames have progressively darker shades. The visualization in Fig. S4 shows that LAV encodes each video as an overall smooth trajectory in the embedding space, where temporally close frames are mapped to nearby points in the embedding space and vice versa. Moreover, corresponding frames from different videos are generally aligned in the embedding space, e.g., points of different colors but similar shades are nearby in the embedding space and vice versa. We also sample one random time-step (highlighted by a black circle), and plot corresponding frames from different videos (each bordered by a distinct color), which are shown to belong to the same action phase. The above observations show the potential application of our self-supervised representation for temporal video alignment.

8. Labels for *Penn Action*

We have made our dense per-frame labels for 2123 videos of *Penn Action* publicly available at https://bit.ly/3f73e2W. Please refer to Tab. 2 of TCC for

Hyperparameter	Value
# of sampled frames (p)	40 (P), 20 (PA, IA)
Batch size	1 (P), 2 (PA, IA)
Learning rate	10^{-4}
Weight decay	10^{-5}
Soft-DTW smoothness (γ)	0.1
Window size (σ)	15 (P, IA), 7 (PA)
Margin (λ)	2
Regularization weight (α)	1.0 (P), 0.5 (PA, IA)
# of context frames (k)	1
Context stride	15 (P, PA), 8 (IA)

Table S6: Hyperparameter settings for LAV. Here, P denotes *Pouring*, PA represents *Penn Action*, and IA denotes *IKEA ASM*. For batch size, 1 means 1 pair of videos (or 2 videos per batch).

more details on actions, numbers of phases, lists of key events, and numbers of videos for training and validation.

9. Implementation Details

For fair evaluations, we use the same data augmentation techniques and encoder networks for all the competing methods. More specifically, we follow the same data augmentation procedures and borrow the encoder networks from TCC [2]. Please refer to the supplementary material of TCC for more details on data augmentation techniques and encoder networks. In addition, we list the hyperparameter settings for our method in Tab. S6. For other methods, we use the same hyperparameter settings suggested by TCC.

References

[1] Ken Chatfield, Karen Simonyan, Andrea Vedaldi, and Andrew Zisserman. Return of the devil in the details: Delving deep into convolutional nets. *arXiv preprint arXiv:1405.3531*, 2014. 2

[2] Debidatta Dwibedi, Yusuf Aytar, Jonathan Tompson, Pierre Sermanet, and Andrew Zisserman. Temporal cycle-consistency learning. In *Proceedings of the IEEE Conference on Computer Vision and Pattern Recognition*, pages 1801–1810, 2019. 2, 4

[3] Laurens van der Maaten and Geoffrey Hinton. Visualizing data using t-sne. *Journal of machine learning research*, 9(Nov):2579–2605, 2008. 3

[4] Ishan Misra, C Lawrence Zitnick, and Martial Hebert. Shuffle and learn: unsupervised learning using temporal order verification. In *European Conference on Computer Vision*, pages 527–544. Springer, 2016. 2

[5] Pierre Sermanet, Corey Lynch, Yevgen Chebotar, Jasmine Hsu, Eric Jang, Stefan Schaal, Sergey Levine, and Google Brain. Time-contrastive networks: Self-supervised learning from video. In *2018 IEEE International Conference on Robotics and Automation (ICRA)*, pages 1134–1141. IEEE, 2018. 2

[6] Dejing Xu, Jun Xiao, Zhou Zhao, Jian Shao, Di Xie, and Yueting Zhuang. Self-supervised spatiotemporal learning via video clip order prediction. In *Proceedings of the IEEE Conference on Computer Vision and Pattern Recognition*, pages 10334–10343, 2019. 3

(a) Baseball Pitch

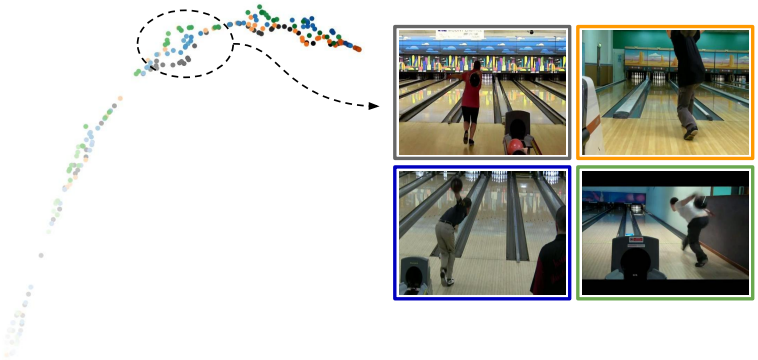

(b) Bowling

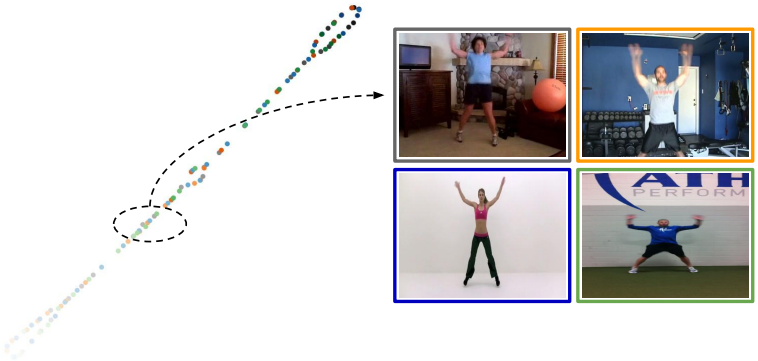

(c) Jumping

Figure S4: Visualization of embeddings for LAV.